Multipotent Retinal Progenitors Express Developmental Markers, Differentiate into Retinal Neurons, and Preserve Light-Mediated Behavior

Henry J. Klassen,[1] *Tat Fong Ng,*[2] *Yasuo Kurimoto,*[2] *Ivan Kirov,*[1] *Marie Shatos,*[2] *Peter Coffey,*[3] *and Michael J. Young*[1]

Purpose. To use progenitor cells isolated from the neural retina for transplantation studies in mice with retinal degeneration.

Methods. Retinal progenitor cells from postnatal day 1 green fluorescent protein-transgenic mice were isolated and characterized. These cells can be expanded greatly in culture and express markers characteristic of neural progenitor cells and/or retinal development.

Results. After they were grafted to the degenerating retina of mature mice, a subset of the retinal progenitor cells developed into mature neurons, including presumptive photoreceptors expressing recoverin, rhodopsin, or cone opsin. In rho$^{-/-}$ hosts, there was rescue of cells in the outer nuclear layer (ONL), along with widespread integration of donor cells into the inner retina, and recipient mice showed improved light-mediated behavior compared with control animals.

Conclusions. These findings have implications for the treatment of retinal degeneration, in which neuronal replacement and photoreceptor rescue are major therapeutic goals. (*Invest Ophthalmol Vis Sci.* 2004;45:4167–4173) DOI:10.1167/iovs.04-0511

Retinal degeneration has many clinically recognized forms and an even greater number of underlying causes.[1,2] A feature common to this heterogeneous group of diseases is photoreceptor loss, resulting in an irreversible decline in visual function. These conditions currently are a substantial source of visual morbidity, and there is a clear need for the development of effective therapeutic strategies. One approach that has been explored is the transplantation of tissue or cells to the diseased eye. Whereas ocular transplantation has long been known to restore visually mediated behavior in lower vertebrates,[3] retinal transplantation initially showed promise in mammals as the result of an experimental approach specifically designed to demonstrate graft–host connectivity. In this model, an embryonic retina transplanted to the brain stem of a rat drove a simple visual function in response to light.[4,5] Efforts to extend this work to intraocular transplants led to clear demonstrations of graft survival and morphologic development, yet persistent difficulty establishing substantial graft–host connectivity.[6–9] The paucity of connections has frequently been attributed to the formation of a reactive glial barrier to regeneration.[10,11] Nevertheless, delayed degeneration of cones after transplantation of cells or tissue to the retina has been reported and is of potential clinical relevance.[12,13]

Transplanted neural progenitor cells have recently been shown to migrate extensively throughout the degenerating mammalian retina, differentiate into neurons, and extend processes into the plexiform and nerve fiber layers, as well as the optic nerve.[14] These findings show the neural progenitor cell (NPC) to be a novel type of donor cell with properties of particular interest in the setting of retinal transplantation. NPCs express a range of markers associated with developmental immaturity, and exhibit multipotency—that is, give rise to the neurons and glia that comprise the respective central nervous system (CNS) compartment from which they are derived.[15–17] In brain and spinal cord, the expected progeny are neurons, astrocytes, and oligodendrocytes. In the retina, the complement of expected neurons specifically includes photoreceptors, whereas the glial population excludes oligodendrocytes. The relevance of compartment-specific lineage considerations to experimental photoreceptor replacement is indicated by the apparent inability of brain-derived progenitors to differentiate fully into mature photoreceptors after transplantation to the mature mammalian retina.[14] In contrast, functional benefits have been reported after the transplantation of brain-derived CNS progenitors to animal models in both brain[18] and spinal cord.[19,20] In the present study, we isolated and characterized multipotent progenitor cells from the neural retina of green fluorescent protein (GFP)-transgenic mice. We examined the expression of retina-specific markers by these cells and evaluated the extent of morphologic integration and host photoreceptor rescue, as well as the impact on visual behavior, after transplantation to the retina of mice with retinal degeneration.

Methods

Mice and Cells

All experiments were performed with strict adherence to the ARVO Statement for the Use of Animals in Ophthalmic and Vision Research, and the Schepens Eye Research Institute Animal Care and Use Committee. C57BL/6 rho$^{-/-}$ mice at 4 weeks of age (n = 12) or C3H rd mice at 4 weeks of age (n = 4), were used as recipients. Retinal progenitor cells (RPCs) were isolated from pooled retinas of postnatal day 1 eGFP transgenic C57Bl/6 mice (gift from Masaru Okabe, University of Osaka, Japan). Retinas were surgically removed, and the ciliary marginal zone and optic nerve head dissected. The tissue was finely minced and digested with 0.1% type I collagenase (Sigma-Aldrich, St. Louis, MO) for 20 minutes. The supernatant containing liberated cells was forced through a 100-μm mesh strainer, centrifuged, and seeded

From the [1]Schepens Eye Research Institute, Department of Ophthalmology, Harvard Medical School, Boston, Massachusetts; the [2]Visual Transplantation Research Group, Department of Psychology, University of Sheffield, Sheffield, United Kingdom; and [3]CHOC Research Institute, Children's Hospital of Orange County, Orange, California.

Supported by The Minda de Gunzburg Research Center for Retinal Transplantation (MJY); the CHOC Foundation, Guilds, and Padrinos (HJK); the Stem Cell Research Foundation (HJK); and the National Eye Institute Grant EY09595 (MJY) and National Institute of Neurological Disorders and Stroke Grant NS044060 (HJK).

Submitted for publication May 7, 2004; revised June 21 and June 29, 2004; accepted July 2, 2004.

Disclosure: **H.J. Klassen**, (P); **T.F. Ng**, None; **Y. Kurimoto**, None; **I. Kirov**, None; **M. Shatos**, None; **P. Coffey**, None; **M.J. Young**, (P)

The publication costs of this article were defrayed in part by page charge payment. This article must therefore be marked "*advertisement*" in accordance with 18 U.S.C. §1734 solely to indicate this fact.

Corresponding author: Michael J. Young, Schepens Eye Research Institute, Department of Ophthalmology, Harvard Medical School, 20 Staniford Street, Boston, MA 02114; mikey@vision.eri.harvard.edu.

into culture vessels in enzyme-inhibiting medium (Neurobasal; Invitrogen-Gibco, Rockville, MD) supplemented with 2 mM L-glutamine, 100 μg/mL penicillin-streptomycin, 20 ng/mL epidermal growth factor (EGF; Promega, Madison, WI), and a neural supplement (B27; Invitrogen-Gibco). This cycle was repeated until all retinal tissue was digested. Cells were refed on alternating days. Within 2 to 3 weeks, RPCs were visible as nonadherent spheres and continued to expand in the presence of EGF. Cultures were split 1:5 every 7 to 10 days. Although capable of expansion through more than 60 passages, cells of less than 20 passages were used in this study.

Differentiation and Characterization of RPCs In Vitro

To examine the differentiation of RPCs in vitro, retinal spheres were seeded onto glass coverslips in the enzyme inhibiting medium containing either EGF or 10% fetal bovine serum (FBS) grown for 1 week and then fixed with 4% paraformaldehyde. Coverslips were blocked in PBS containing 1% bovine serum albumin and Triton X-100 for 30 minutes and incubated with primary antibodies for 2 hours at room temperature. Cells were examined for the following progenitor cell markers: nestin (1:1; DSHB, University of Iowa, Iowa City, IA), Ki-67 diluted (1:100; Vector Laboratories, Burlingame, CA) and for the mature neuronal or retinal markers: MAP2 (1:500; Sigma-Aldrich), NF200 (1:1000; Sigma-Aldrich), GFAP (1:50; Zymed Laboratories, South San Francisco, CA), recoverin (1:2000; gift of Alexander Dhizoor), and rhodopsin (2D4, 1:400, gift of Robert Molday). After incubation with primary antibodies, the coverslips were washed in PBS and then incubated for 1 hour with species-specific IgG conjugated to Cy3 (1:150; Jackson ImmunoResearch Laboratories, West Grove, PA). Coverslips were mounted onto glass slides and visualized by fluorescence microscope (Eclipse; Nikon, Tokyo, Japan).

Reverse Transcription–Polymerase Chain Reaction

Total RNA was extracted using a kit (Purescript RNA Isolation Kit; Gentra, Minneapolis, MN), according to the manufacturer's instructions. The extracted RNA was treated with DNase (DNA-free; Ambion, Austin, TX) to remove any contaminating DNA. Reverse transcription was performed with Moloney murine leukemia virus (M-MLV) reverse transcriptase (Invitrogen, San Diego, CA) using 2 μL RNA in a final volume of 20 μL. Primers were chosen to flank at least one intron whenever possible (see Fig. 3). PCR was performed with 2.7 μL cDNA template, 0.7 μL forward and reverse primers (0.5 μg/μL; Qiagen, Valencia, CA), and 1.25 U *Taq* DNA polymerase (Amersham, Piscataway, NJ) on a thermocycler (Genius; Techne, Princeton, NJ). Four minutes at 94°C was followed by 30 cycles that consisted of 1 minute at 94°C, 1 minute at the annealing temperature corresponding to the primers used (Fig. 3), and 1 minute at 72°C. The final extension reaction was performed for 7 minutes at 72°C. PCR products were visualized on a 2% agarose gel against a 100-bp ladder. Negative controls included RNA, but no reverse transcriptase, to ensure that the PCR product was not amplified from genomic DNA.

Flow Cytometry

Antibodies against CD9, CD15, and CD81 were obtained from BD-Pharmingen (San Diego, CA), as was the PE-conjugated sheep anti-mouse secondary and mineral oil–induced plasmacytoma clone 21 (MOPC) (mouse IgG) used as a control. Anti-GD_2 ganglioside was obtained from U.S. Biological (Swampscott, MA). (Manufacturer's suggested concentrations were used for mAbs, except anti-GD_2 for which 15 μL neat [0.25 mg/mL] was used, based on titration.) After incubation in the dark for 20 minutes, cells were washed with 2 mL PBS and the PE-conjugated secondary added. Samples were allowed to incubate in the dark for an additional 15 minutes and again washed before being resuspended in 200 μL of PBS containing 7-amino actinomycin D (1 μg/mL).

Cell Preparation, Surgery, and Transplantation

Before transplantation, small (50–100 μm diameter) GFP-expressing retinal progenitor spheres were collected, centrifuged at 850 rpm, and resuspended in 200 μL of Hanks' balanced salt solution (HBSS) containing 20 ng/mL EGF.

Mice were deeply anesthetized with an intraperitoneal injection of ketamine (5 mg/kg) and xylazine (10 mg/kg), and the pupils dilated with topical 1% tropicamide to view the fundus. Under transpupillary observation using a binocular surgical microscope, we injected 1 μL HBSS containing RPC neurospheres (approximately 50,000 cells) transsclerally into the subretinal space of the eye, as has been described[21]. Alternatively, mouse fibroblasts ($n = 5$) or the carrier solution alone (sham, $n = 5$) were injected as the control. All injections were made using a beveled glass micropipette (internal diameter, 150 μm) connected by polyethylene tubing to a 50-μL syringe (Hamilton, Reno, NV). We monitored the survival and placement of the grafted cells in vivo by viewing the ocular fundus through a contact lens with a dissecting epifluorescence microscope (Nikon).

Tissue Preparation and Histology

The C3H mice receiving RPC transplants were killed at 4 weeks after transplantation. C57Bl/6 rho$^{-/-}$ mice were used for behavioral assessment and were killed after testing was completed (group 1, 8 weeks; group 2, 25 weeks). The eyes were fixed in 4% paraformaldehyde, cryoprotected in 30% sucrose in 0.1% phosphate buffer, and sectioned at 10 μm on a cryostat. To examine whether the transplants developed into cells expressing photoreceptor markers and to evaluate the survival of host photoreceptors, tissue sections were immunostained for recoverin (a marker for rod and cone photoreceptors and some cone-bipolar cells) rhodopsin (rod photoreceptors), or cone opsin (cone photoreceptors), followed by reaction with Cy3-conjugated secondary antibody. Sections were examined with conventional and confocal microscopy.

Behavioral Testing

Two groups of mice were used in this experiment: Group 1 was examined 8 weeks after transplantation, and group 2 was tested 25 weeks after transplantation. Group 1 contained four congenic eGFP mice, five control-treated rho$^{-/-}$ dystrophic mice, and 8 RPC-transplanted rho$^{-/-}$ dystrophic mice. Group 2 contained two congenic eGFP mice, two control-treated rho$^{-/-}$ dystrophic mice, and four RPC-transplant recipient rho$^{-/-}$ dystrophic mice. In group 1, the control animals received media alone, whereas in group 2 the control animals received fibroblasts. Animals were placed in individual cages with exercise wheels at least 24 hours before testing. The number of wheel revolutions was stored digitally in 10-minute bins. The sequence of testing was as follows: The animals were on 12–12 light–dark cycle. Three hours after the beginning of the dark cycle, a light (150-W halogen bulb) of controlled intensity was presented to all cages.

Statistical Analysis of Behavioral and Anatomic Data

Total exercise wheel running was calculated for the 1-hour period of the light stimulus, and baseline activity calculated for the same circadian period in the absence of a light stimulus. A separate analysis of variance was performed for each group, with factor analysis examined by post hoc Student-Newman-Keuls test.

To quantify photoreceptor survival in rho$^{-/-}$ recipients, we counted recoverin-positive cells in the outer nuclear layer, excluding donor-derived GFP^{+} cells (thus host rods and cones). Photoreceptors were counted within a 16 × 16-μm^2 (256 μm^2) graticule at 40×, and the density of photoreceptors expressed as the number of photoreceptors per square micrometer. A 5 × 5-matrix of photoreceptor density was derived from each retina. Image management software (MatLab; MathWorks, Natick MA) was used to produce the three-dimensional (3-D) figures, with each plot made using the command "surf" performed on the 5 × 5 matrix of photoreceptor or RPC density

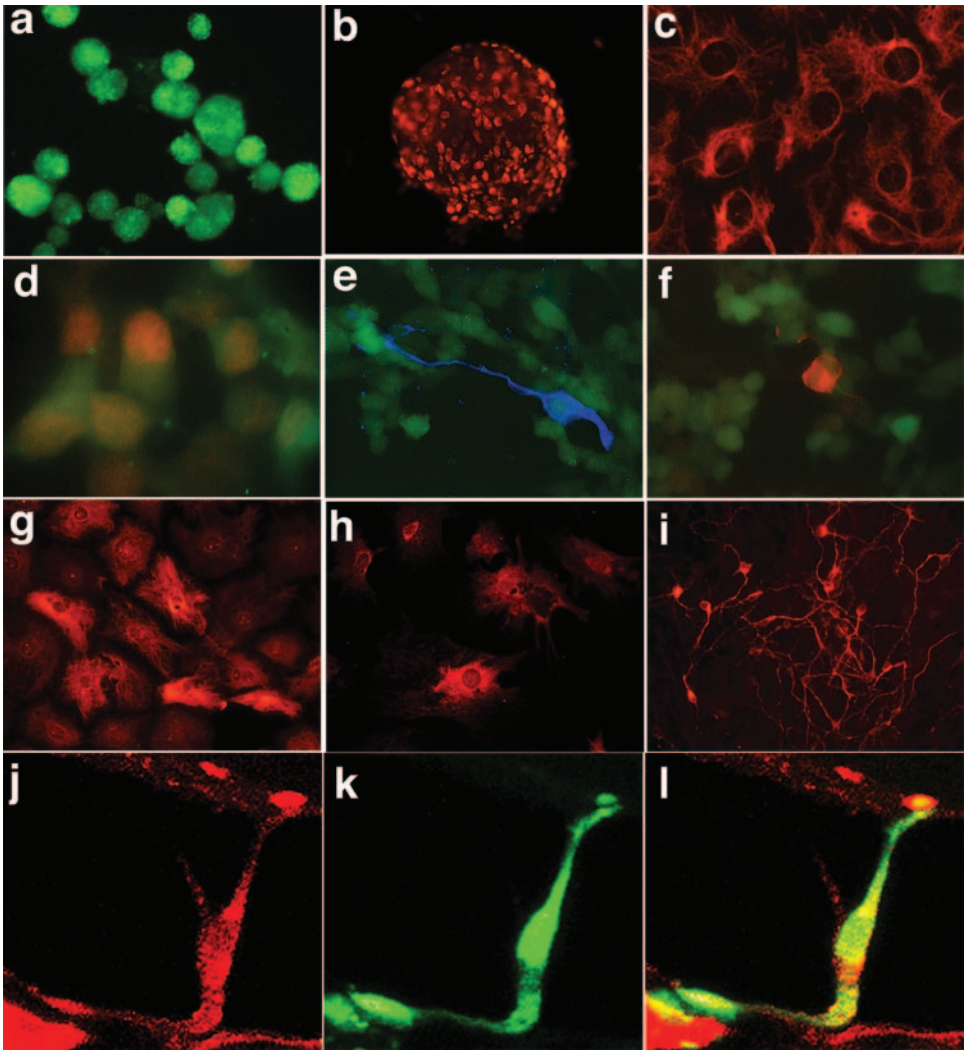

FIGURE 1. Expression of phenotypic markers by GFP$^+$ RPCs. Cultured under proliferation conditions, RPC neurospheres exhibited endogenous GFP (**a**) and widespread immunolabeling for Ki-67 (**b**) and nestin (**c**). Grown as an adherent monolayer, RPCs expressed GFP (**d**, *green*) and widespread nuclear staining for Sox2 (**d**, *red*), with small subpopulations expressing β-III tubulin (**e**, *blue*) and doublecortin (**f**, *red*). (**g–i**) Adherent RPCs cultured under differentiation conditions expressed the mature markers GFAP (**g**), rhodopsin (**h**), and MAP2 (**i**). (**j–l**) Serial images of a transplanted RPC in the dystrophic retina of an rd mouse expressing the retinal photoreceptor marker rhodopsin (**j**, *red*) and GFP (**k**, *green*), with colocalization of these markers shown in the merged image (**l**, *yellow*).

for each eye. Plots were smoothed using the command "shading interp", which interpolates the end or corner values.

To measure the effect of RPC transplantation on photoreceptor survival, we performed a comparison between the density of photoreceptors in the treated right eye versus the untreated left eye in each mouse. Each density value was taken as a sample originating from a Gaussian distribution. Thus, all the 25 sampled values in the right eye had a corresponding sampled value in the left eye. A related-samples *t*-test was performed between the right and left eye distributions to test for a significant difference in their means.

To correlate photoreceptor survival and RPC grafts, photoreceptor density, and mean graft sizes corresponding to the location on the retina were plotted on a two-dimensional graph. A Pearson *r* correlation coefficient was calculated for every mouse with more than 10 nonzero mean graft values. The significance of *r* was calculated for $n = 25$.

RESULTS

Self-renewing progenitor cells can be obtained from the retina of P1 mice. Primary cultures of dissociated GFP-transgenic mouse retina established a population of adherent cells within 24 hours of plating. In the supernatant, nonadherent cellular aggregates (neurospheres) appeared over the initial 5 days and increased in both size and number with time in culture. To investigate the proliferative capacity of the cells comprising these neurospheres, we dissociated them by gentle trituration. This procedure was followed by rapid regeneration of GFP$^+$ neurospheres, consistent with the presence of progenitor cells within the cultured population. Immunofluorescence microscopy of neurospheres revealed not only high levels of sustained GFP expression (Fig. 1a), but also widespread immunolabeling for the proliferation marker Ki-67 (Fig. 1b) and the primitive neuroepithelial marker nestin (Fig. 1c). Immunocytochemical analysis of the adherent population demonstrated widespread nuclear staining for the nuclear transcription factor Sox2 (Fig. 1d), a marker shown to be associated with neural stem cells.[22] In addition, the presence of morphologically distinct subpopulations was revealed by expression of the neuronal marker β-III tubulin (Fig. 1e) and doublecortin (DCX; Fig. 1f), a marker of migrating neuroblasts.[23] Cells staining for these last two markers also exhibited long, thin processes.

Different methods were used to demonstrate that GFP$^+$ RPCs differentiate in culture and in vivo. In the first instance, RPCs were differentiated in culture by 7 days' exposure to 10% FBS (Figs. 1g–i). These cells expressed the mature markers GFAP (Fig. 1g), rhodopsin (Fig. 1h), and MAP2 (Fig. 1i), indicating differentiation along glial, rod photoreceptor, and neuronal lineages, respectively. In the second instance, RPCs were differentiated in vivo by transplantation to the dystrophic retina of rd mice (Figs. 1j–l). In this setting, RPCs continued to express GFP (Fig. 1k), whereas photoreceptor markers including rhodopsin (Fig. 1j) were expressed by many, but not all, grafted cells. In some cases, cells exhibited rod photoreceptor-like morphology together with photoreceptor marker expres-

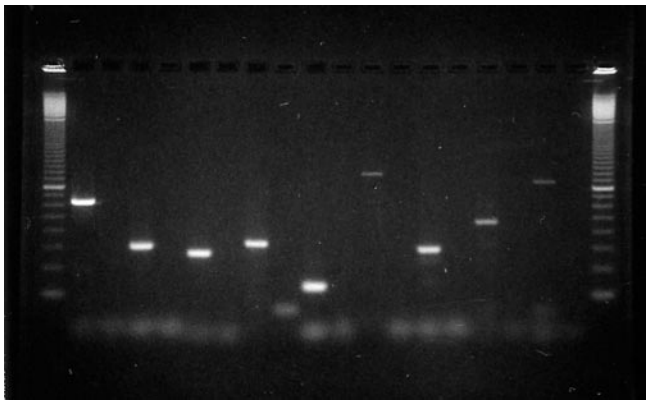

FIGURE 2. Gene expression by GFP^+ RPCs. PCR performed on RNA from GFP^+ RPCs (culture day 40) showed expression of a range of neurodevelopmental genes, including transcripts for (from *left* to *right*) Notch1, Hes1, Hes5, nestin, Sox2, Prox1, Mash1, numb, and NeuroD. Alternating lanes are the negative control, to which no reverse transcriptase was added. The initial lane contains a 100-bp ladder.

sion (Figs. 1j–l). We did not see expression of oligodendrocyte markers by RPCs under any of the experimental conditions.

Examination of cultured RPCs before differentiation revealed expression of neurodevelopmental genes and surface markers. RT-PCR confirmed expression of nestin and Sox2, while also showing expression of other neurodevelopmental genes including Notch1, Hes1, Hes5, Sox2, Prox1, Mash1, numb, and NeuroD (Fig. 2). Flow cytometric analysis demonstrated surface expression of GD_2 ganglioside, CD15 (LeX), and the tetraspanins CD9 and CD81 (Fig. 3).

In $rho^{-/-}$ mice, transplanted RPCs not only integrated into the retina, but rescued host photoreceptors as well. As with rd hosts (Figs. 1j–l, top), RPCs transplanted to $rho^{-/-}$ hosts survived, maintained GFP expression, and migrated throughout the retina (Figs. 4a, 4d–f). The distribution of RPCs revealed migratory preferences for particular retinal layers, with the grafted cells elaborating neuritic arbors appropriate to their location. Comparison of the photoreceptor-containing outer nuclear layer (ONL) between grafted, sham-treated, and untreated $rho^{-/-}$ animals revealed increased ONL thickness in the grafted cohort (Figs. 4a–c). Marker analysis of grafted retinas showed expression of recoverin within the surviving ONL, associated with host profiles as well as donor cells (Fig. 4d). Labeling of cone opsin showed survival of host cones and double-labeling of a small subpopulation (<1%) of donor cells (Fig. 4e). Unlike the findings in rd mice, in $rho^{-/-}$ animals the rod marker rhodopsin was not detected in either grafted RPCs or the host ONL (Fig. 4f).

In terms of function, grafted RPCs conferred visual benefits to $rho^{-/-}$ recipients with retinal degeneration. This was determined with an exercise-wheel test. In this test, normal running behavior in the dark provided the baseline for light-mediated suppression, the threshold intensity of which served as a measure of light sensitivity. For all animals tested, the presentation of a light-stimulus during the dark phase of their diurnal cycle inhibited running in the wheel, with the degree of inhibition contingent on light intensity, degenerative status, and treatment condition. As a positive control, nondystrophic eGFP mice exhibited total suppression of wheel running across all light intensities, except 2.5 ft-c in group 1, compared with their activity during the same period in the dark (Fig. 5a). Untreated dystrophic $rho^{-/-}$ mice showed only significant suppression at the brightest (20 ft-c) level of illumination. In RPC-transplanted animals, suppression was observed across all light intensities and animals in group 1 displayed significantly greater suppression than the sham-operated controls at 10, 5, and 2.5 ft-c illumination ($F = 5.89$ $df = 2,5$ $P < 0.05$), whereas those of group 2 showed significantly greater suppression across all intensities compared with fibroblast-transplanted control retinas ($F = 2.47$ $df = 4,20$ $P < 0.05$).

To examine the anatomy underlying the behavioral results, 3-D retinal maps were generated for treated and control $rho^{-/-}$ mice (Fig. 5b). RPC-transplanted animals in group 1 showed significantly higher maximal photoreceptor density in the grafted right eye (RE) compared with the untreated dystrophic left eye (LE). Similarly, the mean photoreceptor map showed a small region of greater density in the RE than in the LE. In sham-treated control animals, no significant differences in maximum or mean photoreceptor density were observed between eyes. Photoreceptor density was significantly higher in eyes with RPC transplants than in sham-injected eyes. Photoreceptor density was reduced in group 2 compared with the younger animals in group 1, indicative of an ongoing degeneration readily apparent at 25 weeks after transplantation. Over-

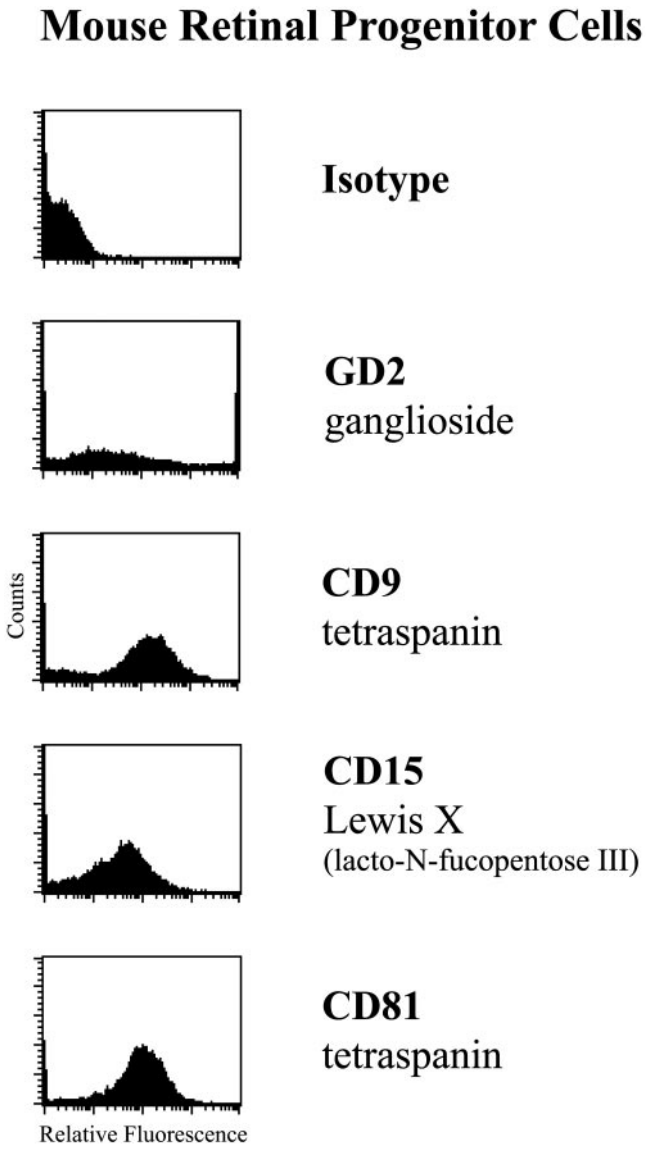

FIGURE 3. Expression of surface markers by GFP^+ RPCs. Flow cytometric analysis of murine RPCs (culture day 60) revealed surface expression of GD_2 ganglioside, CD15 (Lewis X), and the tetraspanins CD9 and CD81, compared with mouse IgG (MOPC; Isotype), used as a negative control.

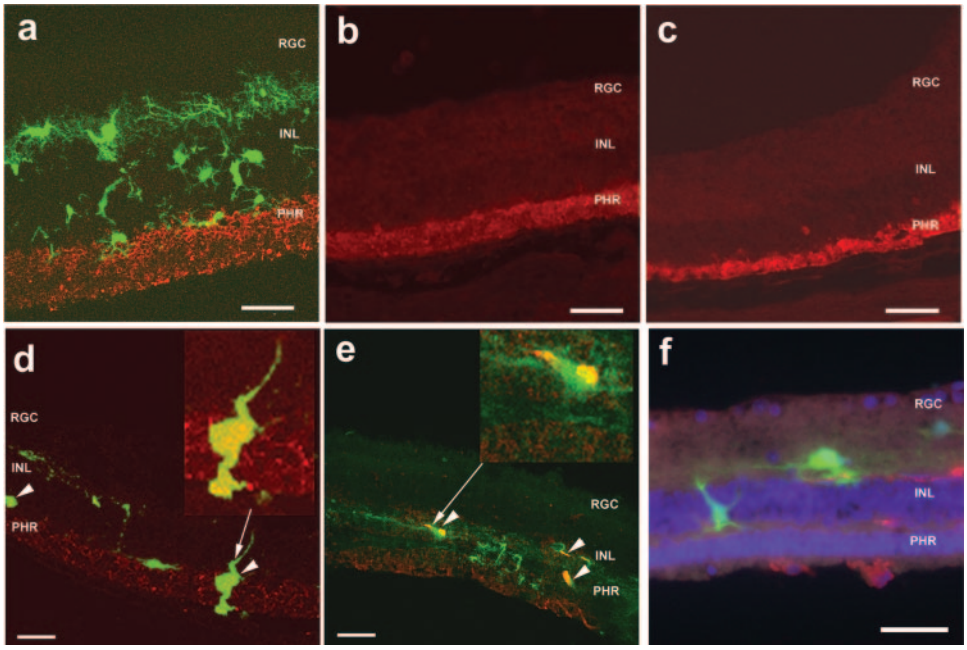

FIGURE 4. Transplantation of GFP$^+$ RPCs and host photoreceptor rescue in rho$^{-/-}$ mice. After transplantation to the subretinal space of dystrophic rho$^{-/-}$ mice, GFP$^+$ RPCs (*green*) preferentially migrated into specific retinal layers and extended cellular processes (**a**, **d**, **e**, **f**). In this model, RPCs migrated to all retinal layers, particularly the INL and adjacent plexiform layers, but only rarely to the ONL or retinal GCL (**d**). The photoreceptor-containing ONL was visualized by recoverin-positive staining (**a**–**d**, *red*) and was thickest in grafted rho$^{-/-}$ retinas (**a**), compared with sham-injected (**b**) or untreated (**c**) littermate retinas. Grafted GFP$^+$ RPCs coexpressed the photoreceptor markers recoverin (**d**, *arrowheads* and *inset*) and cone opsin (**e**, *arrowheads* and *inset*), but did not express rhodopsin (**f**) in the retina of rho$^{-/-}$ hosts (**f**, *blue* stain is 4′,6′-diamino-2-phenylindole [DAPI]).

all, group analysis of RPC-transplanted animals showed no significant differences between eyes in maximum or mean photoreceptor density. Examination of individual animals in the RPC-transplant recipient group revealed small but significant changes in photoreceptor density in some cases, the region of photoreceptor survival being consistent with the location of initial subretinal injection. A significant difference in photoreceptor density was present in the fibroblast control animals, albeit with eyes reversed, apparently due to the deleterious effects of subretinal fibroblasts in the injected RE.

DISCUSSION

In previous work, we showed that transplanted NPCs integrate with the dystrophic retina in a mature rodent.[14] In the present study, we showed the first evidence that a type of NPC, derived from the neural retina, can develop into a photoreceptor after transplantation to retinal dystrophic mice. Specifically, that RPCs expressed recoverin and rhodopsin after transplantation to rd recipients and expressed cone opsin, together with rescuing light-mediated behavior, after transplantation in the rho$^{-/-}$ model. It is important to note that the results obtained

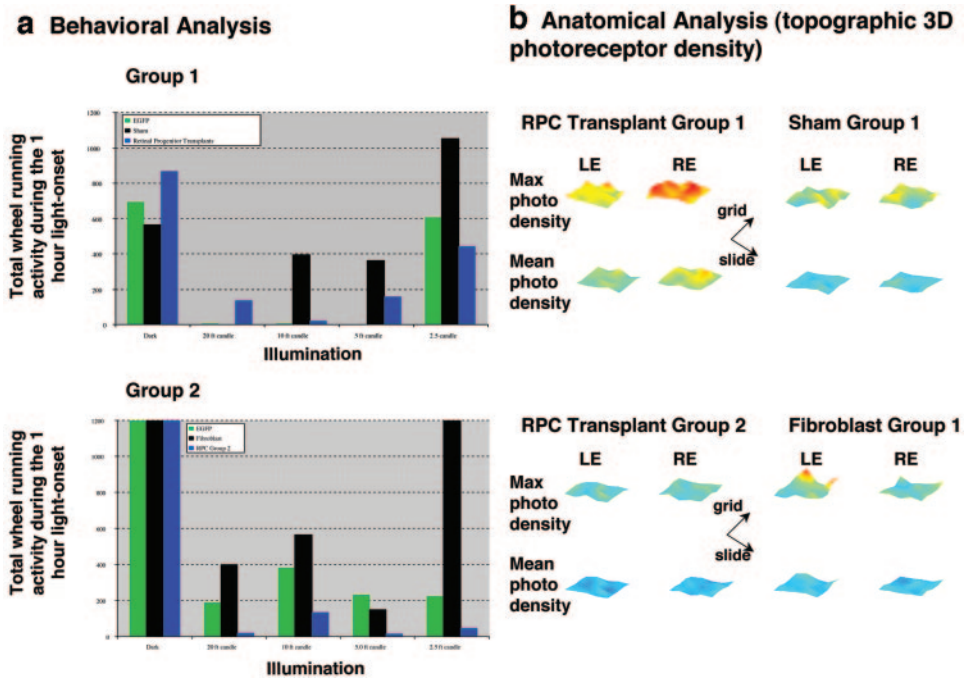

FIGURE 5. Host visual behavior and retinal photoreceptor densities after transplantation of RPCs. Animals in group 1 were examined 8 weeks after transplantation and in group 2 at 25 weeks after transplantation. (**a**) Total number of wheel revolutions (vertical axis) made by mice during a 1-hour exposure to light of the specified intensity (*x*-axis). RPC-recipient dystrophic rho$^{-/-}$ mice (*blue*) exhibited a positive suppression response generally intermediate compared with that of nondystrophic eGFP mice (*green*) and sham-treated rho$^{-/-}$ control animals (*black*) across multiple stimulus levels. The difference between RPC-treated and sham- or fibroblast-treated was particularly significant at the lowest (2.5 ft-c) level. (**b**) 3-D photoreceptor density maps of the treated right eye (RE) versus the untreated left eye (LE) for RPC-recipient and associated sham groups. Both maximum and mean retinal photoreceptor density maps are presented. RPC-recipient animals in group 1 showed significantly higher photoreceptor density in the treated RE, whereas sham-injected control retinas showed no significant differences between eyes. Photoreceptor density was reduced in group 2, consistent with ongoing degeneration at 25 weeks after transplantation. Group analysis of RPC-recipient animals did not show a significant difference between eyes. A significant difference was present in the control animals, with lower photoreceptor density in eyes with fibroblast grafts.

in cultured progenitor cells were not found with either dissociated immature retina[9] or progenitor cells pretreated with the prodifferentiation cytokine ciliary neurotrophic factor (CNTF) (Yau WY, et al. *IOVS* 2004;45:ARVO E-Abstract 5388). In both of these latter situations, migration of donor cells into the retina did not occur, suggesting that the ontogenetic immaturity of CNS progenitor cells is a prerequisite for their migratory behavior and integrative plasticity.

Analysis of gene expression by eGFP-transgenic RPCs provided evidence of their primitive neurodevelopmental status. The gene products detected by immunocytochemistry and RT-PCR have known associations with either neural stem cells or neurogenesis,[22–31] whereas the surface marker pattern detected by flow cytometry is identical with that detected in GFP-transgenic brain progenitors in our previous study.[32] These RPCs therefore appear to be analogous to the progenitor cells studied in of a variety of vertebrates, including fish,[33,34] frogs,[35] birds,[36,37] and mammals.[38–41] The relationship between progenitor cells from the neural retina and the multipotent cells obtained from ciliary epithelium of the eye[42,43] remains to be fully elucidated.

After transplantation to the posterior compartment of the eye, RPCs differentiate into cells of retinal lineage, with expression of recoverin, rhodopsin, or both, in the retina of rd and rho$^{-/-}$ hosts. In the degenerating retina of rd mice, RPCs took up residence in the ONL and in some instances appeared to differentiate into rod photoreceptors. In rho$^{-/-}$ hosts, RPCs migrated extensively, but preferred to integrate in the inner retina, where they exhibited a morphology suggestive of a retinal interneuron. A subpopulation of grafted cells expressed cone opsin; however, we obtained no evidence of differentiation into rhodopsin+ rods in the rho$^{-/-}$ retina. The lack of rod differentiation is puzzling, but may relate to the complete absence of rhodopsin expression in rho$^{-/-}$ hosts. In the apparent absence of injury cues for rod disease, the extensive migration of RPCs to the inner retina may reflect a response to downstream remodeling, including loss of rod bipolar cells, as previously noted in retinal degeneration.[44,45]

RPCs were associated with photoreceptor rescue in the rho$^{-/-}$ retina. The greater thickness of the recoverin-positive ONL in grafted eyes cannot be explained by the presence of space-occupying donor cells, since the majority of GFP^{+} cells were in other layers. Furthermore, rescue was evident in ONL cell counts from which GFP^{+} cells were excluded. In RPC-recipient animals, but not sham-injected controls, photoreceptor density was higher in the treated eye and correlated with graft placement. Graft-associated rescue probably reflects an indirect neuroprotective effect, similar to that reported previously.[19,46–48] There was no evidence of graft rejection in allogeneic rd hosts.[49,50]

The behavioral results indicate that grafted RPCs ameliorate the loss of luminance detection in dystrophic (rho$^{-/-}$) mice at low light levels. Preservation of visual function was observed over a 25-week period, extending into a stage with limited photoreceptor survival. Because the behavioral test is a simple luminance response, the melanopsin system could potentially account for the results. Such effects would, however, tend to be limited to high luminance intensity (20 ft-c), especially at the short time period observed.[51–54] In this study, the sham group did not show suppression of wheel running below that stimulus level, indicating that the behavioral results observed at lower light intensities are a consequence of RPC grafting. How this is achieved is of considerable interest.

Possible mechanisms for the behavioral results could relate to rescue and functional upregulation of host systems or to the addition of new neural circuitry. The present results clearly provide evidence of rod photoreceptor preservation after RPC transplantation and, equally clearly, this does not account for behavioral rescue, because rho$^{-/-}$ rods lack rhodopsin and therefore cannot be functional. In contrast, the possibility of cone rescue and functional upregulation, particularly through an indirect mechanism, deserves consideration.

Mutations in the rhodopsin gene are frequently causative in retinitis pigmentosa, although how this leads to rod photoreceptor death remains unclear. Even less clear is how rod death results in the eventual loss of cones, although the waning of a rod-derived, procone trophic influence has been postulated.[13] In the present study, rod rescue was clearly present. Although rod rescue cannot account directly for the behavioral benefits, this sparing could have long-lasting indirect effects on the cone system. There was also morphologic integration of donor cells in the inner retina, although the functional significance of this phenomenon is not known. The inner retinal reorganization that follows photoreceptor loss resembles a search by the remaining interneurons for synaptic input,[44,45] and it is conceivable that the arrival of highly plastic RPCs results in the creation of more sensitive circuitry, possibly by a higher gain and lower threshold for photic stimuli.

Finally, although we found little evidence for repopulation of the rho$^{-/-}$ ONL with donor-specific photoreceptors, this possibility cannot be entirely discounted, given the advantage in light threshold conferred by even a small number of functional rods. Further work is needed to delineate the scope of CNS progenitor-associated photoreceptor rescue in retinal degeneration models, as well as the degree of synaptic integration and function of engrafted RPCs. Because of the technical difficulties associated with functional assessment in mice, extending this approach to large animal models is of great interest, as it would facilitate the examination of complex visual behavior, including visual acuity. Success in such an endeavor could point the way toward future clinical relevance.

Acknowledgments

The authors thank P. Humphries for the rho$^{-/-}$ mice and Boback Ziaeian, Carlos Gias, and Michael Schwartz for technical assistance. The late J. Wayne Streilein provided valuable intellectual input.

References

1. Bird AC. The Bowman lecture: towards an understanding of age-related macular disease. *Eye*. 2003;17:457–466.
2. Bessant DA, Ali RR, Bhattacharya SS. Molecular genetics and prospects for therapy of the inherited retinal dystrophies. *Curr Opin Genet Dev*. 2001;11:307–316.
3. Stone LS, Zaur IS. Reimplantation and transplantation of adult eyes in the salamander (Triturus viridescens) with return of vision. *J Exp Zoo*. 1940;85:243–269.
4. Klassen H, Lund RD. Retinal transplants can drive a pupillary reflex in host rat brains. *Proc Natl Acad Sci USA*. 1987;84:6958–6960.
5. Klassen H, Lund RD. Retinal graft-mediated pupillary responses in rats: restoration of a reflex function in the mature mammalian brain. *J Neurosci*. 1990;10:578–587.
6. Aramant RB, Seiler MJ. Fiber and synaptic connections between embryonic retinal transplants and host retina. *Exp Neurol*. 1995; 133:244–255.
7. Ghosh F, Bruun A, Ehinger B. Graft-host connections in long-term full-thickness embryonic rabbit retinal transplants. *Invest Ophthalmol Vis Sci.* 1999;40:126–132.
8. Zhang Y, Sharma RK, Ehinger B, Perez MT. Nitric oxide-producing cells project from retinal grafts to the inner plexiform layer of the host retina. *Invest Ophthalmol Vis Sci*. 1999;40:3062–3066.
9. Zhang Y, Arnāer K, Ehinger B, Perez MT. Limitation of anatomical integration between subretinal transplants and the host retina. *Invest Ophthalmol Vis Sci*. 2003;44:324–331.
10. Gouras P, Du J, Kjeldbye H, Yamamoto S, Zack DJ. Reconstruction of degenerate rd mouse retina by transplantation of transgenic photoreceptors. *Invest Ophthalmol Vis Sci*. 1992;33:2579–2586.
11. Kinouchi R, Takeda M, Yang L, Wilhelmsson U, Lundkvist A, Pekny M, Chen DF. Robust neural integration from retinal transplants in

mice deficient in GFAP and vimentin. *Nat Neurosci*. 2003;6:863–868.
12. Mohand-Said S, Hicks D, Dreyfus H, Sahel JA. Selective transplantation of rods delays cone loss in a retinitis pigmentosa model. *Arch Ophthalmol*. 2000;118:807–811.
13. Hicks D, Sahel J. The implications of rod-dependent cone survival for basic and clinical research. *Invest Ophthalmol Vis Sci*. 1999; 40:3071–3074.
14. Young MJ, Ray J, Whiteley SJ, Klassen H, Gage FH. Neuronal differentiation and morphological integration of hippocampal progenitor cells transplanted to the retina of immature and mature dystrophic rats. *Mol Cell Neurosci*. 2000;16:197–205.
15. Weiss S, Reynolds BA, Vescovi AL, Morshead C, Craig CG, van der Kooy D. Is there a neural stem cell in the mammalian forebrain? *Trends Neurosci*. 1996;19:387–393.
16. Gage FH, Ray J, Fisher LJ. Isolation, characterization, and use of stem cells from the CNS. *Annu Rev Neurosci*. 1995;18:159–192.
17. Brustle O, McKay RD. Neuronal progenitors as tools for cell replacement in the nervous system. *Curr Opin Neurobiol*. 1996;6: 688–695.
18. Brèustle O, Jones KN, Learish RD, et al. Embryonic stem cell-derived glial precursors: a source of myelinating transplants. *Science*. 1999;285:754–756.
19. McDonald JW, Liu XZ, Qu Y, et al. Transplanted embryonic stem cells survive, differentiate and promote recovery in injured rat spinal cord. *Nat Med*. 1999;5:1410–1412.
20. Teng YD, Lavik EB, Qu X, et al. Functional recovery following traumatic spinal cord injury mediated by a unique polymer scaffold seeded with neural stem cells. *Proc Natl Acad Sci USA*. 2002;99: 3024–3029.
21. Mizumoto H, Mizumoto K, Whiteley SJ, Shatos M, Klassen H, Young MJ. Transplantation of human neural progenitor cells to the vitreous cavity of the Royal College of Surgeons rat. *Cell Transplant*. 2001;10:223–233.
22. Zappone MV, Galli R, Catena R, et al. Sox2 regulatory sequences direct expression of a (beta)-geo transgene to telencephalic neural stem cells and precursors of the mouse embryo, revealing regionalization of gene expression in CNS stem cells. *Development*. 2000;127:2367–2382.
23. Gleeson JG, Lin PT, Flanagan LA, Walsh CA. Doublecortin is a microtubule-associated protein and is expressed widely by migrating neurons. *Neuron*. 1999;23:257–271.
24. Lendahl U, Zimmerman LB, McKay RD. CNS stem cells express a new class of intermediate filament protein. *Cell*. 1990;60:585–595.
25. Sriuranpong V, Borges MW, Strock CL, et al. Notch signaling induces rapid degradation of achaete-scute homolog 1. *Mol Cell Biol*. 2002;22:3129–3139.
26. Ohtsuka T, Ishibashi M, Gradwohl G, Nakanishi S, Guillemot F, Kageyama R. Hes1 and Hes5 as notch effectors in mammalian neuronal differentiation. *EMBO J*. 1999;18:2196–2207.
27. Ohtsuka T, Sakamoto M, Guillemot F, Kageyama R. Roles of the basic helix-loop-helix genes Hes1 and Hes5 in expansion of neural stem cells of the developing brain. *J Biol Chem*. 2001;276:30467–30474.
28. Morrow EM, Furukawa T, Lee JE, Cepko CL. NeuroD regulates multiple functions in the developing neural retina in rodent. *Development*. 1999;126:23–36.
29. Shen Q, Zhong W, Jan YN, Temple S. Asymmetric Numb distribution is critical for asymmetric cell division of mouse cerebral cortical stem cells and neuroblasts. *Development*. 2002;129:4843–4853.
30. Zhong W, Jiang MM, Schonemann MD, et al. Mouse numb is an essential gene involved in cortical neurogenesis. *Proc Natl Acad Sci U S A*. 2000;97:6844–6849.
31. Dyer MA, Livesey FJ, Cepko CL, Oliver G. Prox1 function controls progenitor cell proliferation and horizontal cell genesis in the mammalian retina. *Nat Genet*. 2003;34:53–58.
32. Klassen H, Schwartz MR, Bailey AH, Young MJ. Surface markers expressed by multipotent human and mouse neural progenitor cells include tetraspanins and non-protein epitopes. *Neurosci Lett*. 2001;312:180–182.
33. Otteson DC, Hitchcock PF. Stem cells in the teleost retina: persistent neurogenesis and injury-induced regeneration. *Vision Res*. 2003;43:927–936.
34. Raymond PA, Hitchcock PF. How the neural retina regenerates. *Results Probl Cell Differ*. 2000;31:197–218.
35. Dorsky RI, Chang WS, Rapaport DH, Harris WA. Regulation of neuronal diversity in the Xenopus retina by Delta signalling. *Nature*. 1997;385:67–70.
36. Fischer AJ, Reh TA. Identification of a proliferating marginal zone of retinal progenitors in postnatal chickens. *Dev Biol*. 2000;220: 197–210.
37. Adler R. A model of retinal cell differentiation in the chick embryo. *Prog Retin Eye Res*. 2000;19:529–557.
38. Jean D, Ewan K, Gruss P. Molecular regulators involved in vertebrate eye development. *Mech Dev*. 1998;76:3–18.
39. Morrow EM, Furukawa T, Cepko CL. Vertebrate photoreceptor cell development and disease. *Trends Cell Biol*. 1998;8:353–358.
40. Ahmad I, Dooley CM, Thoreson WB, Rogers JA, Afiat S. In vitro analysis of a mammalian retinal progenitor that gives rise to neurons and glia. *Brain Res*. 1999;831:1–10.
41. Kelley MW, Turner JK, Reh TA. Regulation of proliferation and photoreceptor differentiation in fetal human retinal cell cultures. *Invest Ophthalmol Vis Sci*. 1995;36:1280–1289.
42. Tropepe V, Coles BL, Chiasson BJ, et al. Retinal stem cells in the adult mammalian eye. *Science*. 2000;287:2032–2036.
43. Ahmad I, Tang L, Pham H. Identification of neural progenitors in the adult mammalian eye. *Biochem Biophys Res Commun*. 2000; 270:517–521.
44. Marc RE, Jones BW, Watt CB, Strettoi E. Neural remodeling in retinal degeneration. *Prog Retin Eye Res*. 2003;22:607–655.
45. Peng YW, Hao Y, Petters RM, Wong F. Ectopic synaptogenesis in the mammalian retina caused by rod photoreceptor-specific mutations. *Nat Neurosci*. 2000;3:1121–1127.
46. Wojciechowski AB, Englund U, Lundberg C, Wictorin K, Warfvinge K. Subretinal transplantation of brain-derived precursor cells to young RCS rats promotes photoreceptor cell survival. *Exp Eye Res*. 2002;75:23–37.
47. LaVail MM, Unoki K, Yasumura D, Matthes MT, Yancopoulos GD, Steinberg RH. Multiple growth factors, cytokines, and neurotrophins rescue photoreceptors from the damaging effects of constant light. *Proc Natl Acad Sci USA*. 1992;89:11249–11253.
48. Whiteley SJ, Klassen H, Coffey PJ, Young MJ. Photoreceptor rescue after low-dose intravitreal IL-1beta injection in the RCS rat. *Exp Eye Res*. 2001;73:557–568.
49. Hori J, Ng TF, Shatos M, Klassen H, Streilein JW, Young MJ. Neural progenitor cells lack immunogenicity and resist destruction as allografts. *Stem Cells*. 2003;21:405–416.
50. Klassen H, Imfeld KL, Ray J, Young MJ, Gage FH, Berman MA. The immunological properties of adult hippocampal progenitor cells. *Vision Res*. 2003;43:947–956.
51. Panda S, Provencio I, Tu DC, et al. Melanopsin is required for non-image-forming photic responses in blind mice. *Science*. 2003; 301:525–527.
52. Mrosovsky N, Foster RG, Salmon PA. Thresholds for masking responses to light in three strains of retinally degenerate mice. *J Comp Physiol*. 1999;184:423–428.
53. Mrosovsky N, Salmon PA, Foster RG, McCall MA. Responses to light after retinal degeneration. *Vision Res.* 2000;40:575–578.
54. Hattar S, Lucas RJ, Mrosovsky N, et al. Melanopsin and rod-cone photoreceptive systems account for all major accessory visual functions in mice. *Nature*. 2003;424:75–81.